Nuclear Medicine and Biology 42 (2015) 711–719

Contents lists available at ScienceDirect

Nuclear Medicine and Biology

journal homepage: www.elsevier.com/locate/nucmedbio

Exploration of the impact of stereochemistry on the identification of the novel translocator protein PET imaging agent [^{18}F]GE-180

Wai-Fung Chau [a], Andrew M.A. Black [a], Alan Clarke [b], Clare Durrant [a], Ingvil Gausemel [b], Imtiaz Khan [a], Dimitrios Mantzilas [b], Inger Oulie [b], Astri Rogstad [b], William Trigg [a], Paul A. Jones [a,*]

[a] GE Healthcare, The Grove Centre, White Lion Road, Amersham, Buckinghamshire, HP7 9LL, UK
[b] GE Healthcare AS, Nycoveien 1-2 Postboks 4220 Nydalen, Oslo, 0401, NO

ARTICLE INFO

Article history:
Received 9 December 2014
Received in revised form 8 May 2015
Accepted 20 May 2015

Keywords:
[^{18}F]GE-180
PET radiotracer
Imaging TSPO
Chiral stability
In vitro and *in vivo* metabolites
Biodistribution

ABSTRACT

Introduction: The tricyclic indole compound, [^{18}F]GE-180 has been previously identified as a promising positron emission tomography (PET) imaging agent of the translocator protein (TSPO) with the potential to aid in the diagnosis, prognosis and therapy monitoring of degenerative neuroinflammatory conditions such as multiple sclerosis. [^{18}F]GE-180 was first identified and evaluated as a racemate, but subsequent evaluations of the resolved enantiomers have shown that the *S*-enantiomer has a higher affinity for TSPO and an improved *in vivo* biodistribution performance, in terms of higher uptake in specific brain regions and good clearance (as described previously). Here we describe the additional biological evaluations carried out to confirm the improved performance of the *S*-enantiomer and including experiments which have demonstrated the stability of the chiral centre to chemical and biological factors.
Materials and Methods: GE-180 and the corresponding radiolabelling precursor were separated into single enantiomers using semi-preparative chiral supercritical fluid chromatography (SFC). A detailed comparison of the individual enantiomers and the racemate was carried out in a number of biological studies. TSPO binding affinity was assessed using a radioligand binding assay. Incubation with rat hepatic S9 fractions was used to monitor metabolic stability. *In vivo* biodistribution studies up to 60 min post injection (PI) in naïve rats were carried out to monitor uptake and clearance. Achiral and chiral *in vivo* metabolite detection methods were developed to assess the presence of metabolite/s in plasma and brain samples, with the chiral method also determining potential racemisation at the chiral centre.
Results: Evaluation of the chiral stability of the two enantiomers to metabolism by rat S9 fractions, showed no racemisation of enantiomers. There were notable differences in the biodistribution between the racemate and the *R*- and *S*-enantiomers. All compounds had similar initial brain uptake between 0.99 and 1.01% injected dose (id) at 2 min PI, with *S*-[^{18}F]GE-180 showing significantly greater retention than the *R*-enantiomer at 10 and 30 min PI ($P < 0.05$). *S*-[^{18}F]GE-180 uptake to the TSPO-expressing olfactory bulbs was 0.45% id (SD ± 0.17) at 30 min PI in comparison to *RS*-[^{18}F]GE-180 or *R*-[^{18}F]GE-180 levels of 0.41% id ±0.09 and 0.23% id ±0.02 respectively, at the same timepoint ($P > 0.05$). The signal-to-noise ratio (ratio olfactory bulb to striata binding) were similar for both *RS*-[^{18}F]GE-180 and *S*-[^{18}F]GE-180 (3.2 and 3.4 respectively). Initial uptake to the lungs (an organ with high TSPO expression) was more than 3-fold greater with *S*-[^{18}F]GE-180 than *R*-[^{18}F]GE-180, and significantly higher at 10 and 30 min PI ($P < 0.05$). Furthermore lung uptake of *S*-[^{18}F]GE-180 at 2 and 10 min PI was also significant when compared to the racemate ($P < 0.05$).
The majority of the radioactivity in the rat brain following administration of *RS*-[^{18}F]GE-180 or *S*-[^{18}F]GE-180 was due to the presence of the parent compound (91% ± 1.5 and 94% ± 2.0 of total radioactivity at 60 min PI respectively). In contrast at 60 min PI for the plasma samples, the parent compounds accounted for only 28% ± 1.2 and 21% ± 4.6 of total radioactivity for *RS*-[^{18}F]GE-180 and *S*-[^{18}F]GE-180 respectively. Chiral assessment confirmed that the *S*-enantiomer was chirally stable *in vivo*, with no stereochemical conversion in brain and plasma samples up to 60 min PI.
Conclusions: Developing racemic radiotracers, as for racemic therapeutics, is a considerable challenge due to differences of the enantiomers in pharmacokinetics, efficacy and potential toxicity. We have shown that the enantiomers of the promising racemic PET ligand [^{18}F]GE-180 do not share identical performance, with *S*-[^{18}F]GE-180 demonstrating higher TSPO affinity, higher brain uptake and better retention to the high TSPO-expressing lungs. Furthermore, *S*-[^{18}F]GE-180 has also been shown to be enantiomerically stable *in vivo*, with no observed conversation of the eutomer to the distomer. As a single enantiomer, *S*-[^{18}F]GE-180 retains the beneficial characteristics of the racemate and is a promising imaging agent for imaging neuroinflammation *in vivo*.

* Corresponding author at: GE Healthcare Life Sciences, The Grove Centre, White Lion Road, Amersham, Buckinghamshire HP7 9LL, UK.
E-mail address: PaulJones@ge.com (P.A. Jones).

http://dx.doi.org/10.1016/j.nucmedbio.2015.05.004
0969-8051/

1. Introduction

Translocator protein (TSPO) is an 18 kDa, five transmembrane domain protein formerly known as the peripheral benzodiazepine receptor (PBR). It is primarily located within the outer membrane of the mitochondria where it forms a part of a multimeric complex along with the 32 kDa voltage-dependent anion channel, and the 30 kDa adenine nucleotide translocase [1]. TSPO is involved in steroidogenesis, whereby TSPO mediates cholesterol transport into mitochondria [2–6], but the precise functions of TSPO during neuroinflammation are not yet fully understood. There is however a significant increase in TSPO expression in immune cells (ostensibly microglia) as part of the neuroninflammatory cascade that follows a cerebral insult [7].

The correlative relationship between increased TSPO expression and neuroinflammation has in recent years led TSPO to be the main target for imaging neuroinflammation [8]. [^{11}C]-*R*-PK11195 was the first of the non-benzodiazepine and selective TSPO radioligands that was clinically established [9] and has been used in many clinical and pre-clinical PET studies. Whilst [^{11}C]-*R*-PK11195 has been employed in many informative studies of immune cell activation, it is not an ideal PET imaging tracer [10]. Therefore, in recent years there has been a desire to find new improved *in vivo* TSPO PET and single photon emission computer tomography (SPECT) ligands with improved pharmacokinetic properties. As a result, there have been several new promising ligands that have been identified and evaluated [11–13]. We have evaluated several different classes of TSPO ligands, which have led to the development of new potential TSPO tracers (includes: diaryl anilide, tetracyclic and tricyclic indole classes) [14–16]. Here we will describe more extensively the investigation and evaluations which identified *S*-[^{18}F]GE-180 as a promising TSPO imaging candidate [14].

GE-180 has a single chiral centre and was first synthesised and evaluated as a racemate (Fig. 1). GE-180 was separated into *S*- and *R*- isomers, and the absolute stereochemistry of each was determined using vibrational circular dichroism (VCD) spectroscopy [17]. Since it has been known that enantiomers may have different pharmacokinetic, pharmacodynamics and safety/toxicity profiles compared to that of its racemate form [18,19] further experiments on the individual stereoisomers were essential. In pharmacology, the activity of racemic drugs can be divided into three main groups: 1 — Racemic drugs with one major bioactive enantiomer, 2 — racemic drugs with equally bioactive enantiomers or 3 — racemic drugs with chiral inversion. Often, it is the case of one enantiomer containing all of the desired bioactivity (known as the eutomer) with the other enantiomer, the distomer being less active (group 1). In some extreme cases, the individual enantiomers have markedly different and extreme effects (such as for Thalidomide where one enantiomer is effective against nausea for pregnant women and the other teratogenic for the unborn foetus; see [19] for review). On the whole, a single enantiomer is preferable than its racemate form, as to ensure the best performance as a radiotracer. In general single enantiomer drugs reduce the potential for complex drug interactions, have less complex pharmacokinetic profiles, less complex relationships between plasma concentration and effect as well as a potential for an improved therapeutic index [18]. Since, the chiral stability of the active enantiomer of the related tetracyclic class of the TSPO ligands was previously evaluated and showed good stability during radiosynthesis and in formulation but rapid racemisation in plasma [16], it was crucial to demonstrate the stability of *S*-[^{18}F]GE-180 (of the tricyclic class) in biological media. Hence the individual enantiomers of [^{18}F]GE-180 were prepared and investigated in a series of biological tests. The key biological considerations are essentially metabolic stability, specific binding and ligand receptor kinetics (i.e. brain uptake and washout). Fig. 2 shows the assessment approach adopted in this study.

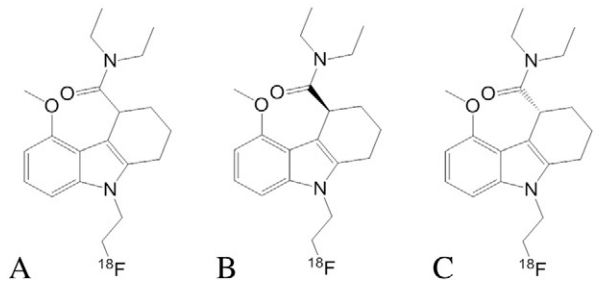

Fig. 1. The molecular structures of [^{18}F]GE-180 (A) racemate: (*RS*)-*N*,*N*-diethyl-9-(2-[^{18}F]fluoroethyl)-5-methoxy-2,3,4,9-tetrahydro-1*H*-carbazole-4-carboxamide and its enantiomers (B) *S*-enantiomer: (*S*)-*N*,*N*-diethyl-9-(2-[^{18}F]fluoroethyl)-5-methoxy-2,3,4,9-tetrahydro-1*H*-carbazole-4-carboxamide *S*-enantiomer and (C) *R*-enantiomer: (*R*)-*N*,*N*-diethyl-9-(2-[^{18}F]fluoroethyl)-5-methoxy-2,3,4,9-tetrahydro-1*H*-carbazole-4-carboxamide.

The affinities and the regional brain biodistribution data of the racemate and both its enantiomers were published previously in brief [14], however the exact steps and method have been described in further details in this paper.

2. Materials and methods

2.1. Synthesis and radiosynthesis of [^{18}F]GE-180

Unlabelled GE-180 and the corresponding mesylate radiolabelling precursor was prepared according to the methods previously published [14,20] and resolved to the single enantiomers using supercritical fluid chromatography (SFC) to give materials with >99% enantiomeric excess (ee). [^{18}F]GE-180 was manufactured on a FASTlab platform with [^{18}F] Fluoride supplied from a GE Healthcare PET cyclotron. Kryptofix 222 (K2.2.2) (4 mg, 10.6 μmol), potassium bicarbonate (10 μmol) and acetonitrile (0.5 mL) were added to [^{18}F]F^-/H_2O (ca. 400 MBq, 100–300 μL) in a cyclic olefin copolymer (COC) reaction vessel. The mixture was dried by heating at 100 °C under a stream of nitrogen for 20–25 minutes. After drying and without cooling, the mesylate precursor compound (*S*)-2-(4-(diethylcarbamoyl)-5-methoxy-3,4-dihydro-1H-carbazol-9(2H)-yl)ethyl methanesulfonate (1 mg, 1.5–3 μmol) in acetonitrile (1 mL) was added to the COC reaction vessel and heated at 100 °C for 10 minutes. After cooling, the reaction mixture was removed and the COC reaction vessel rinsed with water (1.5 mL) and the rinsate added to the main crude reaction. Following this, the crude product was applied to a semi-preparative HPLC system (Hichrom ACE 5 C18 column (5 μm, 100 × 10 mm internal diameter; 100 Å, particle size 5 μm); mobile phase (50% water and 50% acetonitrile) were delivered at a flow rate of 3 mL/min; UV detector set to a detection wavelength of 254 nm). The [^{18}F]GE-180 fraction was then diluted to a volume of 10 mL with water and adsorbed on a tC18 Sep-Pak (lite) cartridge (pre-conditioned with 2 mL of ethanol followed by 5 mL of water-for the low radio-activity preparation). The cartridge was washed with water (2 mL), and eluted in the final formulation with anhydrous ethanol (0.5 mL) followed with Dulbecco's phosphate buffered saline (PBS at 4.5 mL), physiological pH 6–9. Radioactivity was measured using a radioisotope dose calibrator (Capintec CRC-15R).

High activity radiosysntheses were also prepared depending on the study demand on the study day. For the higher activity radiosynthesis preparations from a starting activity of approximately 40GBq, the above steps were carried out but with the added steps of using ascorbic acid as a radio-stabiliser in the following: HPLC eluent (as 0.1 mg/mL ascorbic acid in water), 20 mL PBS containing 20 mg ascorbic acid HPLC vial) and to pre-condition the tC18 cartridges (as a 1 mg/mL in 5 mL solution in water). The radiolabelled molecules were purified by HPLC prior to the biological evaluations, using a Chromolith RP-18E 100 × 4.6 mm column with water and methanol on a gradient method.

Chiral HPLC analysis of the radiolabelled compounds was carried out to determine if any racemisation had occurred during radio-synthesis. The effect of changing the reaction temperature on the chiral integrity of the synthesis was also evaluated. Both reducing and increasing the reaction temperature and heating duration were assessed. Reaction

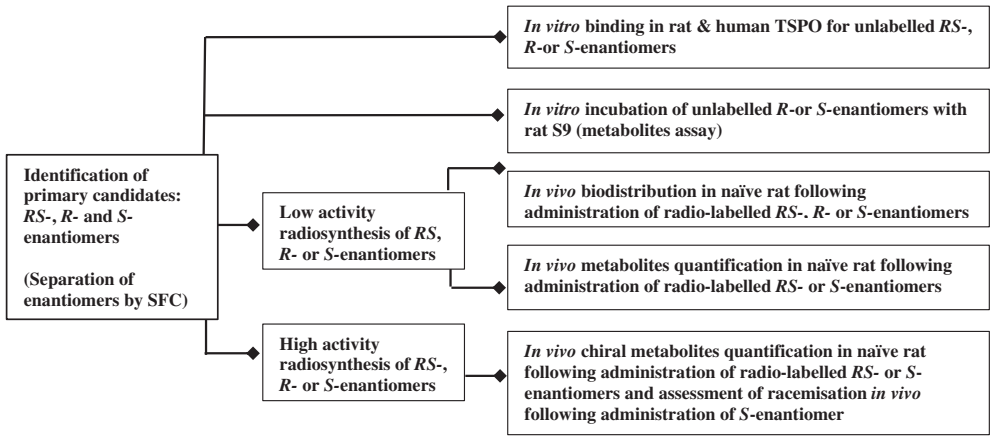

Fig. 2. Assessment approach.

parameters of 130 °C/30 min and 80 °C/15 min were compared with the standard reaction conditions of 100 °C/15 min.

2.2. Separation of the enantiomers by SFC

The racemate was resolved into its individual enantiomers by SFC [21]. One hundred milligrams of the *RS*-GE-180 crude were dissolved with minimal volume of 1.4-dioxane, resulting in up to 40 mg/mL stock solutions. The combined fractions from the SFC purifications had the organic solvents removed by evaporation at 40 °C, to form a film. The film was dissolved by first adding 15 mL acetonitrile and then 30 mL Milli-Q water, before the flasks were frozen using dry ice and acetone. After the solution was frozen both flasks were freeze dried using a Sentry 2.0 freeze dryer. Separation was carried out, by the use of a Kromasil Amycoat 250 × 10 mm 5 μm, 100 Å column at 40 °C under isocratic conditions (20% isopropyl alcohol over a 10 min run at a flow of 1.4 mL/min). Enantiomeric purity determination was carried out by a chiralpak IC (cellulose *tris*(3,5-dichlorophenyl)carbamate based), 250 × 4.6 mm, 5 μm, column (from Chiral Technologies) under isocratic conditions (80% water:20% methanol v/v) at 1 mL/min flow rate over a 20 min run.

2.3. In vitro affinity

This method involved a competition binding assay of the racemate, *R*- and *S*-enantiomers binding to Wistar rat heart TSPO (n = 2 for all compounds) against 0.3 nM [^{3}H]PK11195 (reference) using an adapted method from Le Fur et al. [22]. Reactions were carried out in 50 mM Tris-HCL (pH 7.7) 10 mM $MgCl_2$ and incubated in 1% DMSO at 25 °C for 15 min, with the reaction terminated by rapid vacuum filtration of the contents onto glass fibre filters. The radioactivity collected was then compared to those of the control values in order to ascertain any interactions of the test compounds with the TSPO binding site. In addition, the three compounds were run against human TSPO (human colonic cell membranes), whereby reactions were carried out at room temperature, and in rat kidney membranes (0–4 °C) for 60 min. In general, each non-radioactive test compound was screened at 12 different concentrations (n = 2).

2.4. In vitro metabolites

Unlabelled *S*-GE-180 and *R*-GE-180 were spiked into plasma samples and were incubated for up to 4 hours at 37 °C to study *in vitro* chiral stability. Unlabelled *S*-GE-180 (~25 μL) was also incubated with S9 rat liver fractions (~200 μL), containing tris-HCL buffer (~575 μl) and beta-nicotinamide adenine dinucleotide phosphate, β-NADPH (~200 μL) for up to 4 hours at 37 °C to study potential racemisation. In brief, 100 μL aliquots of the test mixture samples (duplicates) after incubation were added to ice cold acetonitrile and ethanol (left over night in the fridge for protein precipitation), mixed and then centrifuged. The supernatant was then subsequently evaporated to dryness by N_2-gas and then the dried extracts re-dissolved in acetonitrile (100 μL). HPLC analysis was then performed on the processed samples, using an online Solid Phase Extraction (SPE) cartridge (LiChrospher ADS RP-4, 25 × 4 mm, 25 μm) and then a chiral column (Chiralpak IC 0.46 × 25 cm) using a UV/visible detector (at 230 nm). Elution was by a gradient method using 10 mM ammonium acetate in acetonitrile and methanol over a 41 minute run with a flow of 500 μL/min. The samples incubated in S9, were also analysed on the same chromatograph equipped with a Waters XBridge Shield RP18 2.5 μm, 4.6 × 50 mm column. A gradient of 10 mM ammonium acetate and acetonitrile over a gradient for 12 min was applied, at a flow of 500 μL/min.

2.5. In vivo biodistribution studies

All animal experiments were carried out in compliance with the Animals (Scientific Procedures) Act 1986 act, and all regulated procedures within this study were carried out by qualified personnel. All animals were allowed at least 3 days acclimatisation in the animal housing unit before being included in the study.

Naïve male Sprague Dawley rats weighing ~ 200–250 g were administered with approximately 1 to 3 MBq of the test compound per animal. The tracers were injected intravenously via a tail vein in a volume of approximately 0.1 to 0.3 mL. A total of 6 animals were used at each of the 2, 10, 30 and 60 min post injection (PI) timepoints over two study days. Sacrifice was by cervical dislocation while under gaseous anaesthesia (with 4% isoflurane in oxygen). Immediately after sacrifice, the brains were removed and dissected. Other organs, tissue and excreta were also dissected and assayed for radioactivity using a purpose-built gamma counter (the hardware for the counter was commissioned to Gravatom Engineering Systems and the software to Solcom; the counter was capable of assessing whole organs and provides counts for the entire animal). The decay corrected percentage of injected dose (% id) for each sample was calculated. For blood, bone, muscle, skin and fat, where representative samples were collected, appropriate body composition factors were applied for these tissue samples in order to calculate the % id in the entire tissue. All the other tissues, organs and excreta, were collected intact at dissection and the % id calculated as a percentage of the total radioactive dose administered. Activity of the regionally dissected brain samples were measured on a Wallac gamma counter before being combined and included as a whole brain sample on the purpose-built gamma counter. *In vivo* biodistribution was carried out for *RS*-[^{18}F]GE-180, *S*-[^{18}F]GE-180 and *R*-[^{18}F]GE-180 (n = 2–6).

2.6. In-vivo metabolites (for the achiral analysis)

Male Wistar rats (~200 g bodyweight) were anaesthetized using isoflurane (4% isoflurane in oxygen). In separate studies, *RS*-[^{18}F]GE-180 and *S*-[^{18}F]GE-180 was intravenously injected as a bolus via a tail vein at a radioactive dose of approximately 20 MBq in 1 mL. The rats were allowed to recover from the anaesthesia, and then at the point of sacrifice (10, 30 or 60 min PI), the rats were further anaesthetised and then sacrificed by cervical dislocation. One animal was used for the 10 and 30 min PI timepoints, whereas for the 60 min PI samples, the plasma or brain tissues from two animals were combined, to ensure adequate radioactivity due to the short half-life cycle. A total of three studies containing these timepoints were carried out on three separate study days. Blood was collected from the vena cava, transferred to a Vacutainer (pre-coated with Ethylenediaminetetraacetic acid anticoagulant), mixed, transferred to an eppendorf tube and then centrifuged at 3500 × *g* for 3 min to obtain plasma. The brain was removed from the skull and the cerebellum, medulla and pons discarded. All samples were immediately transferred on wet ice for sample clean up (protein precipitation) prior to HPLC analysis. Although different rat strains were used in the metabolism studies than for the biodistribution studies, both Wistar and Sprague Dawley rats are from the same main class of outbred albino stocks. This is considered to have minimal impact on the validity of the study, which were focused on the distribution and metabolism of GE-180 in a naïve animal expressing low (normal) levels of TSPO.

2.6.1. Preparation of in-vivo samples for HPLC analysis (for the achiral analysis)

Plasma samples from each of the time-points above were added to ice cold 100% acetonitrile in a 1:10 volume per volume (v/v) ratio and centrifuged at 132000 rpm (approximately 16000 × *g*) for 3 min to allow for protein precipitation. Similarly the brain sample was homogenized with ice-cold acetonitrile (10 mL per brain sample) using a rotary blade homogeniser at maximum speed for approximately 1 min, followed by centrifugation at 5000 rpm (approximately 4500 × *g*) for 5 min. For both plasma and brain samples, following centrifugation the supernatant was removed by rotary evaporation at 40 °C, followed by reconstitution of the plasma pellet with 2.5 mL of mobile phase (60% acetonitrile and 40% water). The resulting sample was then passed through a 0.22 μm low protein binding filter to remove particulates prior to HPLC injection. Radioactivity was assayed using a gamma counter at each stage to monitor extraction recoveries.

2.6.2. HPLC analysis by the achiral method

HPLC was used to analyse the radiochemical profile of the metabolites and the parent peak. A 1 mL aliquot of sample (after protein precipitation) was manually injected into a Rheodyne injector and analysed using a C_{18} semi-preparative 7.8 × 300 mm; 10 μm;125 Å μBondapak column (Waters), with a C_{18} Vydac 218 TD 5 μm guard cartridge (Grace). Analysis was carried with an isocratic method with 60% HPLC grade water (mobile phase A) and 40% HPLC grade acetonitrile (mobile phase B) running over a 20 min run time at a flow rate of 3 mL/min (from a binary pump). The separation was performed at ambient temperature. Radioactivity detection was via a dual Bismuth Germanate (BGO) coincident radioactive detector with a 500 μL loop and a bioscan flow count. The ultraviolet (UV) absorbance was captured with an UV/Vis detector set at a wavelength of 230 nm with an absorbance unit full scale (AUFS) of 0.1. A universal chromatography interface (UCI) was used to convert the electronic signal to digital data. The Chromeleon HPLC software (version 6.6 Dionex) was used for data acquisition and integration. The area under the curve of the parent peak from the radio trace represented the radio chemical purity (RCP). The parent peak of the tracer of interest in each study was verified on the HPLC profiles by co-injection with the corresponding non-radioactive compound i.e. by retention time comparison.

2.7. In-vivo metabolites (chiral analysis)

Approximately 40 MBq (in 1 mL) of *RS*-[^{18}F]GE-180 or *S*-[^{18}F]GE-180 was administered intravenously to male Wistar rats (~200 g) using the same procedure and timepoints as mentioned previously in the achiral methodology. Sample processing followed by HPLC analysis was then carried out. The *RS* compound was analysed once on the chiral set-up (Fig. 7 traces A, D and E) simply to show elution order of the isomers. The *R*-[^{18}F]GE-180 injection was similarly analysed only once on the system, to further verify the approximate retention time of this isoform. The *S*-enantiomer (compound of interest) was analysed in triplicate (example chromatographs Fig. 7 traces B, F and G), to show repeatability. Single injections of both the *RS*- compound and *R*-enantiomer were considered sufficient for the purpose of verifying that this methodology was capable of detecting both isoforms.

2.7.1. Preparation of in vivo samples for HPLC analysis (by chiral analysis)

Similar to the achiral methodology, all the biological samples prior to HPLC analysis were processed to remove proteins and phospholipids from the sample matrix. This is especially important with the use of a chiral column, due to its sensitivity to overloading affecting column usage. The protein precipitation for the brain samples for chiral analysis was carried out in the same way as described for the samples subjected to achiral analysis above, with the exception that the mobile phase used for re-constitution was 85% methanol and acetonitrile (50/50 v/v) and 15% 10 mM ammonium acetate.

However for plasma samples three stages of sample processing were carried out (Fig. 3). A mixture of ice-cold methanol and acetonitrile (50%:50% v/v) was used as the extraction solvent with a 1:10 v/v ratio of plasma to solvent being used and centrifuged at 132000 rpm (approximately 16000 × *g*) for 3 min to allow for protein precipitation. After protein precipitation 0.4 mL of the reconstituted sample was filtered through a Mini Uniprep system (GE Healthcare Whatman) to further eliminate particulate matter. The filtrate was then placed onto the auto sampler for injection on to the final online SPE clean up stage. Similarly for the achiral method, aliquots were measured for radioactivity on the gamma counter at each stage to account for extraction recoveries.

2.7.2. HPLC analysis by the chiral method

A chiral HPLC method was developed and optimised to primarily assess potential racemisation of *S*-[^{18}F]GE-180 *in vivo*. In addition, *RS*-[^{18}F]GE-180 was also analysed to demonstrate that the methodology was capable of detecting both forms of enantiomers. The method consisted of an online solid SPE clean up (the final clean up stage after filtration using the mini uni-prep system), followed by a chiral separation method. The same radio- and UV-detection set-up was used as with that of the achiral method but with a smaller sample loop of 200 μL in the BGO detector. A 16 min gradient run programme was performed at a flow rate of 1 mL/min (Table 1) using degassed and filtered buffers (mobile phase A = 10 mM ammonium acetate and B = 50%

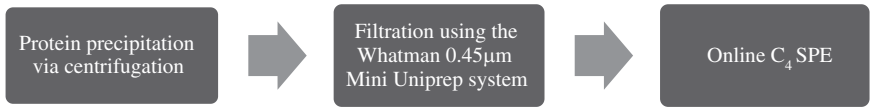

Fig. 3. The three stages of plasma sample clean up prior to chiral HPLC analysis.

Table 1
SPE (pump 1) and chiral column gradient programme (pump 2) with valve set up state.

Time (min)	Pump 1		Pump 2		Valve state	Description
	% Mobile phase A	% Mobile phase B	% Mobile phase A	% Mobile phase B		
0	90	10	60	40	Load	SPE load stage; chiral column equilibration
2	90	10	60	40	Inject	SPE back flushed on to chiral column
2.5	15	85	15	85	N/A	N/A
5.5	15	85	15	85	Load	SPE re-conditioning; sample separation on chiral column
6.1	90	10	N/A	N/A	N/A	N/A
9.0	90	10	N/A	N/A	N/A	N/A
9.5	0	100	N/A	N/A	N/A	N/A
13.0	0	100	N/A	N/A	N/A	N/A
13.5	90	10	5	95	N/A	N/A
14.2	N/A	N/A	0	100	N/A	N/A
16.0	90	10	60	40	N/A	N/A

N/A = not applicable.

acetonitrile and 50% methanol v/v) from two binary pumps. A switching valve was used to operate the flow direction of the eluents from both pumps at various stages. Three stages to the SPE process were carried out with the use of a pre-programmed switching valve. The first stage involved the loading of the processed sample (50 μL through a 50 μL polyether ether ketone (PEEK) sample loop by the use of an auto-sampler) onto the C4 SPE cartridge (LiChrospher RP-4 ADS; 25 μm; 4 mm × 25 mm, 60 Å, pH range 2–7), to concentrate and to retain the analytes of interest. The C4 cartridge allows for the retainment of the more hydrophobic species i.e. the parent peak. The next stage, involved the back-flushing of the previously retained analytes of interest from the SPE onto the connecting chiral column (Chiralpak IC 5 μm; 4.60 × 250 mm, Daicel) attached to a pre-guard cartridge (Chiralpak IC 5 μm; 4.0 × 10 mm, Daicel). The final stage, involved the separation of the compound of interest and its metabolites on the chiral column and SPE re-equilibration, ready for the subsequent injection.

In general, the hydrophilic analytes of interest were captured on the hydrophobic bonded phase of the sorbent in the SPE cartridge using low organic levels (pump 1). After sample loading onto the SPE, the direction of the flow was changed, with the valve state switched to 'inject'. The organic phase (mobile phase B) was then increased to a high level and remained constant at this level for a few minutes to allow for sufficient back flushing of the retained analytes from the SPE onto the connecting chiral column. In parallel during the SPE loading stage, the chiral column undergoes equilibration (operated by pump 2). After the analytes have transferred onto the analytical column, the valve was switched back to its original 'load' position, and the analyte separation was carried out over a gradient (with pump 2 pumping mobile phase onto the analytical column). Meanwhile, pump 1 underwent its own cycle of clean up and re-equilibration. A summary of both gradients used and the synchronisation of the two pumps are described in Table 1 with a schematic of the mobile phase flow direction illustrated in Fig. 4. Recoveries were verified at each stage and were deemed sufficient (>70% recovery).

2.8. Statistical analysis

Where appropriate, data are presented as mean ± standard deviation (SD). Two way analysis of variance (ANOVA) was used to compare the *in vivo* biodistribution of the three compounds across the timepoints in the individual organs and tissues. Where ANOVA indicated a significant difference, a *post hoc* Student t-test (unpaired; Prism) compared the groups, and statistical significance was considered where $P < 0.05$.

3. Results and discussion

3.1. Radiochemistry

For the lower-activity radiosyntheses of *S*-[^{18}F]GE-180 the radiochemical yield was 26% (based on n = 8) non-decay corrected with a process time of 90 minutes, and the radiochemical purity (RCP) was >99% in all preparations. For the higher-activity radiosyntheses (for *S*-[^{18}F]GE-180) the end of synthesis yields were typically 7 to 12% (non-decay corrected based on n = 2). Before biological evaluation,

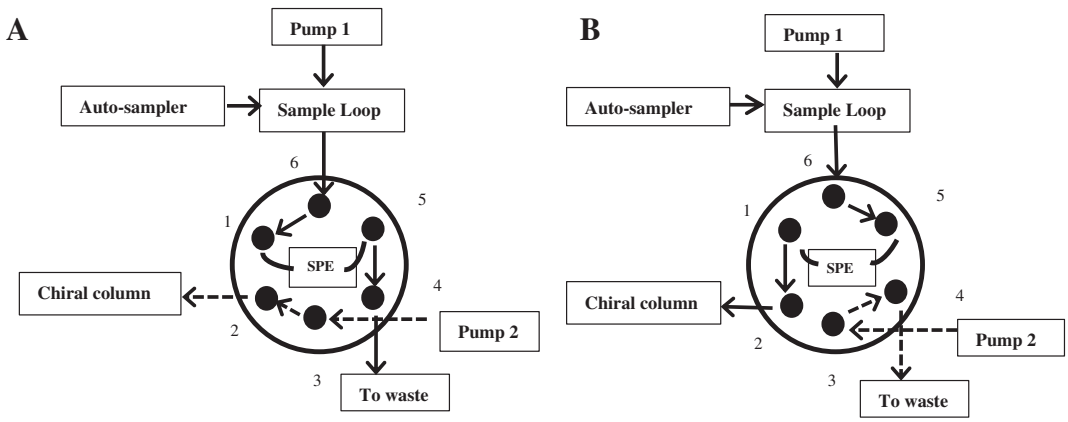

Fig. 4. Schematic of a Rheodyne valve showing the mobile phase flow direction from two pumps to the SPE cartridge and to the chiral column. a) Load state: Sample loading onto SPE by pump l via valve at port 6 and port 1, with non-retained material being washed through to port 5, 4 and then to waste (solid line); Chiral column equilibration by pump 2 via port 3, port 2 and then to waste (dashed line). b) Inject state (60 degree rotation of 6-port valve): In this position, the flow was reversed from port 5 with eluent back flushing the previously retained analytes from the SPE to port 1, then 2 and finally onto the chiral column and injection onto the connecting chiral column followed by separation operated by pump 1 (solid line). Simultaneously, pump 2 flushes mobile phase B to waste via port 3 and 4 (dashed line).

samples were purified, and the RCP was found to be an average of >90%. A higher radioactivity was required for the chiral metabolism method, to compensate for the less volume per concentration injected onto the HPLC and the overall longer sample processing time required. Significant degradation to the mesylate precursor to the corresponding alcohol and vinyl impurities was observed as a result of heating, as expected with the higher temperature/longer time duration (130 °C/30 min) compared to the lower temperature and shorter time duration setting (80 °C/15 min).

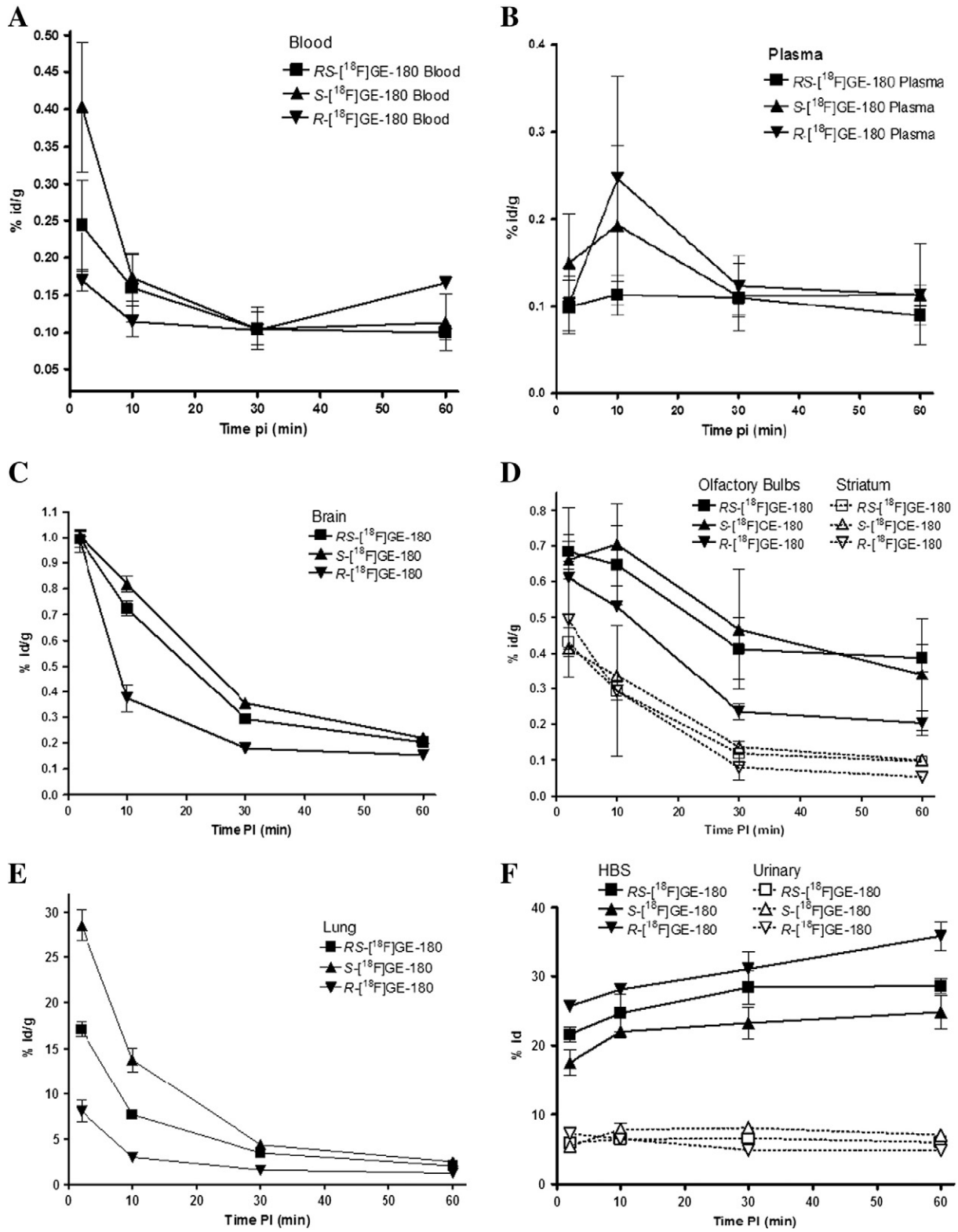

Fig. 5. Biodistribution data comparing % radioactivity in key organs and tissues after administration of 1-3 MBq of *RS*-[^{18}F]GE-180 (n = 3–6; specific activity 4–21 Gbq/μmol). *S*-[^{18}F]GE-180 (n = 3–6; 10–22 GBq/μmol) or *R*-[^{18}F]GE-180 (n = 2–3; 83 GBq/μmol) in naïve Sprague Dawley rats at 2, 10, 30 and 60 min PI. Error bars = standard deviation. HBS = hepatobiliary system.

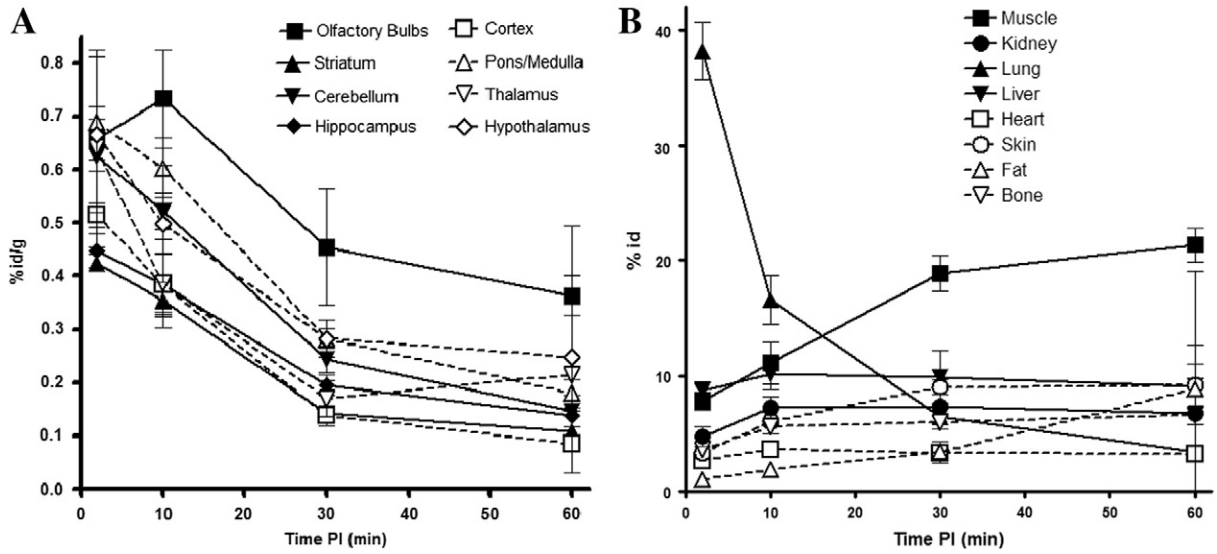

Fig. 6. Biodistribution of *S*-[^{18}F]GE-180 in A) key brain regions B) other organs in Sprague Dawley rats at 2, 10, 30 and 60 min PI (n = 3–6). For further details see Fig. 5 legend.

End of synthesis yield of 20% and 11% were obtained respectively, with 99% ee and >99% radiochemical purities obtained on all accounts.

3.2. In vitro affinity

In rat heart, *S*-GE-180 was found to be more potent, with an Ki of 0.87 nM, ~4.4 fold higher than the less active *R*-GE-180 enantiomer with a Ki of 3.87 nM as previously reported [14]. The affinity for *S*-GE-180 correlated well with *RS*-GE-180 (Ki 0.59 nM). In human, the results were similar in terms of potency order with *S*-GE-180 (9.2 nM) being the most potent, followed by *RS*-GE-180 (11.5 nM) and then *S*-GE-180 (14.1 nM).

3.3. In vitro metabolites

Racemisation of the test compound in plasma would be inferred by the presence of the opposite enantiomer. Following chiral HLPC analysis, only the parent peak was observed for each of the test compounds, demonstrating stability of the enantiomers in plasma. Racemisation of the more active *S*-GE-180 enantiomer was also not observed after incubation with the rat S9 liver fraction i.e. the *S*-GE-180 enantiomer does not racemise to *R*-GE-180. Low levels of unidentified polar metabolites (7%) were observed after 4 hours incubation in both enantiomers.

3.4. In vivo biodistribution

Following intravenous administration, *S*-[^{18}F]GE-180 displayed the most rapid radioactivity clearance from blood at early timepoints, followed by the racemate and then *R*-[^{18}F]GE-180 (Fig. 5A). A steady-state level (~0.1% id/g) by 30 min was reached for all three test compounds, except for *R*-[^{18}F]GE-180, which increased to 0.2% id/g levels at 60 min PI. In general there was lower uptake in the plasma samples at the initial timepoint compared to blood, which similarly reached a steady state level of approximately 0.1% id/g by 30 min (for all three compounds) (Fig. 5B). Brain uptake of >0.5% id/g by 2 min for TSPO central nervous system (CNS) tracers is considered desirable [23]. Although this uptake was exceeded by all three compounds, with similar whole brain uptake of between 0.99 and 1.01% id (equivalent to 0.51 to 0.53 id/g) at 2 min PI (Fig. 5C), the retention of *S*-[^{18}F]GE-180 was significantly greater than *R*-[^{18}F]GE-180 by 10 min PI, with activity levels remaining higher for as long as 30 min PI ($P < 0.05$). The washout (rate of initial brain uptake at 2 min compared to brain uptake in subsequent timepoints) was fast for all three compounds with no significant difference ($P > 0.05$; Fig. 5C). The ability to penetrate the blood brain barrier (BBB) and have fast washout kinetics are highly desirable properties for a useful brain imaging agent; a criteria met by all the [^{18}F]GE-180 compounds. The difference in tracer retention between the high TSPO expressing olfactory bulbs and the low expressing striata have been used as the basis for determining specific signal uptake to non-specific clearance of potential TSPO binding imaging agents, as previously described [14]. The more active *S*-[^{18}F]GE-180 demonstrated OB retention at 30 min PI of 0.45% id compared to *RS*-[^{18}F]GE-180 of 0.41% id and *R*-[^{18}F]GE-180 of 0.23% id ($P > 0.05$). Clearance from the non-selective regions (striata) was rapid and reached a steady state by approximately 30 min PI (Fig. 5D), with all three compounds showing similar clearance. The olfactory bulb/striata ratios (indicative of specific to non-specific binding) were also similar and in the order of *S*-[^{18}F]GE-180 (3.2), *RS*-[^{18}F]GE-180 (3.4) and *R*-[^{18}F]GE-180 (2.9). The organ with the highest initial uptake at 2 min was to the lungs (example Fig. 6A); this was consistent with other selective TSPO ligands, as is the subsequent rapid clearance in this organ by 30 min PI in all three test compounds (Fig. 5E) ($P < 0.05$ for *S*-[^{18}F]GE-180 versus *R*-[^{18}F]GE-180 at

Table 2
Mean total relative percentage of parents and metabolites ± standard deviation (by achiral HPLC analysis) in Wistar rats after administration of *RS*-[^{18}F]GE-180/*S*-[^{18}F]GE-180 (~20 MBq) sacrificed at 10, 30 & 60 min PI (n = 3).

Sample	Species	*RS*-[^{18}F]GE-180 Mean total relative % ± SD			*S*-[^{18}F]GE-180 Mean total relative % ± SD		
		10 min PI	30 min PI	60 min PI	10 min PI	30 min PI	60 min PI
Brain	Parent	100	97 ± 1.0	91 ± 1.5	98 ± 1.7	96 ± 2.6	94 ± 2.0
	Metabolites	0	3 ± 1.0	9 ± 1.5	2 ± 1.7	4 ± 2.6	6 ± 2.1
Plasma	Parent	81 ± 3.5	49 ± 12.5	28 ± 1.2	70 ± 18.2	41 ± 16.2	21 ± 4.6
	Metabolites	19 ± 3.5	51 ± 12.5	72 ± 1.2	30 ± 18.1	59 ± 16.4	79 ± 4.6

Specific activity was between 3 and 82 GBq/μmol.

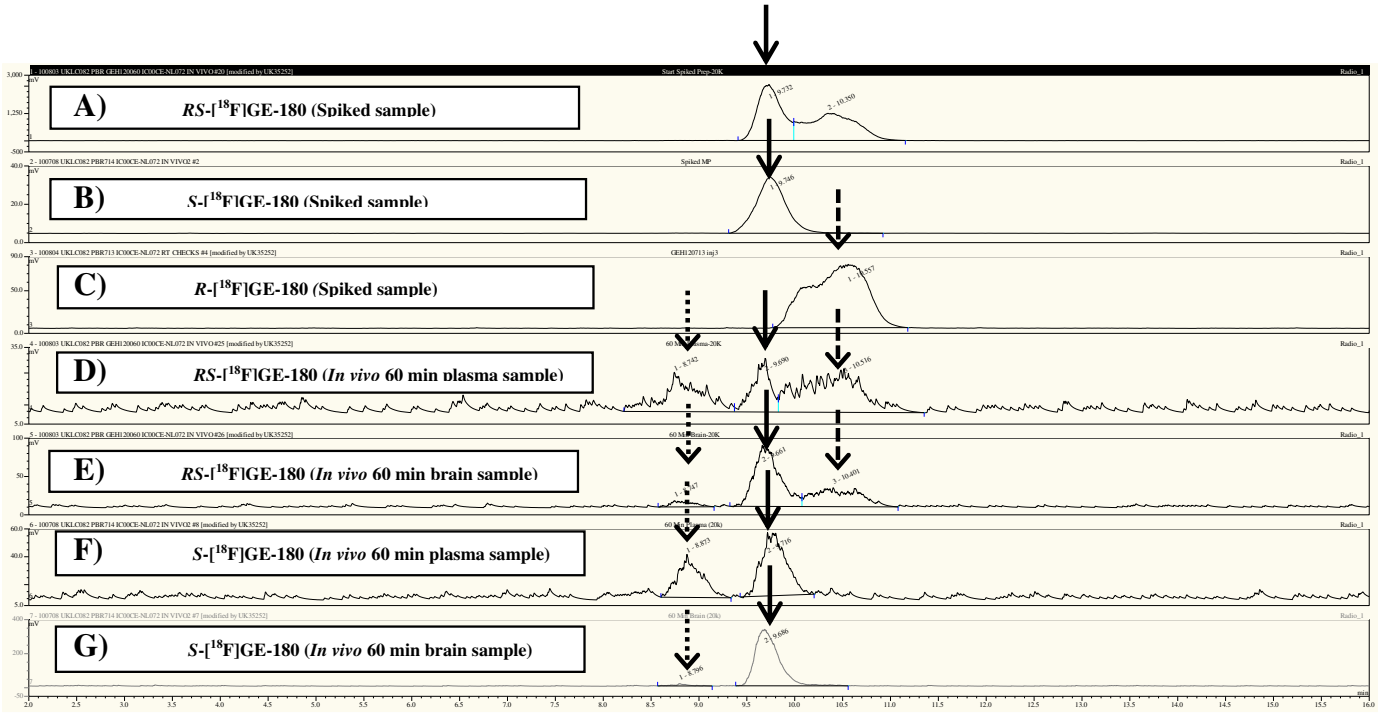

Fig. 7. Example radio-HPLC chromatograms showing the elution order of the *S*-enantiomer followed by the *R*-enantiomer in both *in vivo* samples (traces E, F & G) and spiked (*ex vivo*) samples (traces A,B & C), with a metabolite species obtained in the 60 min *in vivo* plasma and brain samples. The HPLC chromatographs show a response of millivolts (mV) on the y axis and time (min) on the x axis. The numbers displayed on the top of each peak shows the peak numbering followed by the retention time. Chromatograms were not decayed corrected, but samples were injected onto the HPLC as soon as possible in each instance. In this study, spiked sample refers to mobile phase spiked with the radiolabelled compound of interest). Where applicable, the *S*-, *R*- and metabolite peaks are represented by a solid, dash and square dot arrows respectively. The retention times of the metabolite, *S*- and *R*- peaks were consistently ~8.8, ~9.8 & ~10.5 min respectively. The reduced signal/noise ratio observed in the 60 min plasma samples (Fig. 7 D and F) was as expected due to the limited amount of radioactivity injected onto the HPLC as a result of the extra sample processing stage used. One hydrophilic non-parent peak was observed in the 60 min plasma and brain samples following *RS*-compound injection (Fig. 7D), since the run time of this peak was different to that of the *S*-enantiomer (Fig. 7B), this was confirmed to be the metabolite and not the parent peak.

2, 10 and 30 min PI and for *S*-[^{18}F]GE-180 versus *RS*-[^{18}F]GE-180 at 2 and 10 min PI). Excretion for all test compounds was primarily via the hepatobiliary system (HBS), with activity contained within the liver, intestines and faeces. Urinary excretion accounted for a smaller % id than HBS, irrespective of the timepoint (Fig. 5F). In brief, the biodistribution data show the single *S*-enantiomer, *S*-[^{18}F]GE-180 to have comparable properties to the racemate and supports the single *S*-enantiomer as the lead candidate.

The highest TSPO expressing region in the rat brain are the olfactory bulbs, with one of the lowest expressing regions being the striatium (Fig. 6A). The general distribution (Fig. 6B) shows the lung displaying the greatest uptake compared to the other organs at the earlier timepoints of 2 and 10 min PI only (e.g. muscle, kidneys, liver, heart, skin and fat). In addition, bone activity levels also increased slightly with time from 3.66% id to 6.49% id at 2 and 60 min PI respectively for *S*-[^{18}F]GE-180 (not shown). Due to the expressions of TSPO on haematogenous cells, this is likely to be due to selective retention to the bone marrow as opposed to the accumulation of free radiolabelled fluoride [24].

3.5. Achiral in vivo metabolites

The *in vivo* metabolic profile of both *RS*-[^{18}F]GE-180 and *S*-[^{18}F]GE-180 was assessed in brain and plasma using non-chiral reverse phase radio-HPLC. For an imaging agent targeted at the CNS it is important that the signal in the brain is attributable to the parent molecule and not to radiolabeled metabolite/s. In the *S*-[^{18}F]GE-180 brain sample, there was only minimal presence of metabolite species, with 98 ± 1.7% and 94 ± 2.0% parent detected at 10 and 60 min PI respectively. In the plasma, the amount of radioactivity attributable to *S*-[^{18}F]GE-180 was 70 ± 18.2% and 21 ± 4.6% of the total activity at the same timepoints (Table 2). Similar results were observed following the administration of *RS*-[^{18}F]GE-180 (Table 2). Across the timepoints evaluated for *S*-[^{18}F]GE-180, only three metabolites were observed in the brain samples, all of which were more hydrophilic than the parent compound, with the most hydrophilic metabolite species typically being the most prominent (not shown). The three hydrophilic metabolite species identified in the brain (at very low proportions) were likely to be those identified in the

Table 3
The average % activity of *R*- and *S*-enantiomers or metabolites at 10, 30 and 60 min PI in brain and plasma of Wistar rats injected with only *S*-[^{18}F]GE-180 (~40 MBq) and analysed by chiral HPLC (n = 3).

% Composition after *S*-[^{18}F]GE-180	Plasma			Brain		
	10 min PI	30 min PI	60 min PI	10 min PI	30 min PI	60 min PI
% total metabolites	16 ± 7.1	35 ± 9.7	37 ± 4.2	0	0	0.7 ± 1.2
% *S*-[^{18}F]GE-180	84 ± 7.1	65 ± 9.7	63 ± 4.2	100	100	99 ± 1.2
% *R*-[^{18}F]GE-180	0	0	0	0	0	0

Specific activity was between 33 and 588 GBq/μmol.

plasma (based on similar HPLC run times). There was no novel metabolite in the brain that was not observed at higher respective levels in the plasma, suggesting that the brain metabolites are formed in the periphery and have poor BBB permeability.

At the earliest timepoint (10 min) there was little evidence of significant amounts of metabolites in the brain (no metabolites were detected for the racemate and no more than 2% in total for the *S*-enantiomer). Thirty minutes PI in the rat is the most relevant time point that would equate to the expected human imaging time [25]. At that time in the rat, there is very low proportion of metabolites detected in the brain (3–4% of the radioactivity) for the racemate and *S*-enantiomer respectively. This equates to an extremely low amount of material (~0.01% total % id) due to 3–4% total relative radioactivity associated with metabolites in 0.30 and 0.36% of injected dose in the rat brain at that time for *RS*-[^{18}F]GE-180/*S*-[^{18}F]GE-180 respectively. For the *S*-enantiomer at 60 min, only a total of 0.01% of injected dose (6% of 0.22% id) is present as metabolites in the brain (due to the low amount of total activity in the brain at this timepoint; see Fig. 5C). The fact that there was a slightly higher proportion of metabolites in the brain at this later time point (6% at the final timepoint as compared to 2% at the initial time point) suggests that the metabolite(s) may be capable of crossing the BBB, and this process is slower than for *S*-enantiomer itself. However the low levels of the metabolites in the plasma at the early time point (10 min PI) and the slower transport across the BBB is indicative that metabolites are not likely to impact brain uptake or retention to such an extent as to result in poorer imaging qualities. Table 2 shows the total relative percentage of parents and metabolites determined by achiral HPLC.

3.6. Chiral in vivo metabolites

RS-[^{18}F]GE-180 or *S*-[^{18}F]GE-180 were intravenously administered into male Wistar rats, with brain and plasma samples at 10, 30 and 60 min PI assessed by chiral reverse phase chromatography, for the presence of the *R*-enantiomer. Peaks corresponding to both *S*-[^{18}F]GE-180 and *R*-[^{18}F]GE-180 (based on retention times) were present after injection of *RS*-[^{18}F]GE-180, verifying that the method was capable of detecting both stereoisomers (Fig. 7 trace E). The *R*-[^{18}F]GE-180 peak was not detected after injection of *S*-[^{18}F]GE-180, indicating that racemisation did not take place *in vivo* (Fig. 7 trace G). Peaks that were not associated with the retention times of either the *R*- or/and *S*-enantiomers were attributed to metabolites (Table 3). Representative analytical radiochromatograms comparing the *RS*-, *S*- and *R*-enantiomers by chiral HPLC analysis are shown in Fig. 7 trace A–G. In general the brain samples from the chiral *in vivo* method were comparable to that of achiral HPLC analysis with no or minimal metabolites observed throughout the 60 min timepoint duration.

4. Conclusions

The development of racemic compounds for radiolabelled diagnostic tracers or therapeutic drugs is extremely challenging due to the likelihood of differences between the individual enantiomers (as exemplified by the extreme and catastrophic differences in the pharmacology of the eutomer and distomer of thalidomide). As well as differences in toxicological profile, enantiomers can also have disparity in pharmacokinetics and target affinity. For radiolabelled PET tracers this would complicate the image processing required, with any algorithm having to model for the *in vivo* behaviour of the radioactivity associated with 2 differently behaving compounds. Furthermore, due to the lessons learned from experiences with drugs like thalidomide, the pathway for regulatory approval of racemates is considerably more difficult than single enantiomeric compounds. [^{18}F]GE-180, a promising radiolabelled agent for TSPO imaging by PET, is a chiral compound with two enantiomers. This study has demonstrated that these enantiomers do not share identical performance. The *S*-[^{18}F]GE-180 has an affinity for TSPO that is 1.5- to 4-fold better than the *R*-enantiomer in rat heart and has both higher brain uptake and greater retention to the high TSPO-expressing lungs when injected iv to rats. Furthermore, *S*-[^{18}F]GE-180 has also been shown to be enantiomerically stable *in vivo*, with no observed conversation of the eutomer to the distomer. As a single enantiomer, *S*-[^{18}F]GE-180 retains the beneficial characteristics of the racemate and is a promising imaging agent for imaging neuroinflammation *in vivo*.

References

[1] McEnery MW, Snowman AM, Trifiletti RR, Snyder SH. Isolation of the mitochondrial benzodiazepine receptor: association with the voltage-dependent anion channel and the adenine nucleotide carrier. Proc Natl Acad Sci U S A 1992;89:3170–4.
[2] Papadopoulos V, Amri H, Boujrad N, Cascio C, Culty M, Garnier M, et al. Peripheral benzodiazepine receptor in cholesterol transport and steroidogenesis. Steroids 1997;62:21–8.
[3] Casellas P, Galiegue S, Basile AS. Peripheral benzodiazepine receptors and mitochondrial function. Neurochem Int 2002;40:475–86.
[4] Scarf AM, Kassiou M. The translocator protein. J Nucl Med 2011;52:677–80.
[5] Papadopoulos V, Miller WL. Role of mitochondria in steroidogenesis. Best Pract Res Clin Endocrinol Metab 2012;26:771–90.
[6] Rupprecht R, Papadopoulos V, Rammes G, Baghai TC, Fan J, Akula N, et al. Translocator protein (18 kDa) (TSPO) as a therapeutic target for neurological and psychiatric disorders. Nat Rev Drug Discov 2010;9:971–88.
[7] Chen MK, Guilarte TR. Translocator protein 18 kDa (TSPO): molecular sensor of brain injury and repair. Pharmacol Ther 2008;118:1–17.
[8] Venneti S, Lopresti BJ, Wiley CA. The peripheral benzodiazepine receptor (translocator protein 18 kDa) in microglia: from pathology to imaging. Prog Neurobiol 2006;80:308–22.
[9] Chauveau F, Boutin H, Van Camp N, Dolle F, Tavitian B. Nuclear imaging of neuroinflammation: a comprehensive review of [11C]PK11195 challengers. Eur J Nucl Med Mol Imaging 2008;35:2304–19.
[10] Ching AS, Kuhnast B, Damont A, Roeda D, Tavitian B, Dolle F. Current paradigm of the 18-kDa translocator protein (TSPO) as a molecular target for PET imaging in neuroinflammation and neurodegenerative diseases. Insights Imaging 2012;3:111–9.
[11] Miyoshi M, Ito H, Arakawa R, Takahashi H, Takano H, Higuchi M, et al. Quantitative analysis of peripheral benzodiazepine receptor in the human brain using PET with (11)C-AC-5216. J Nucl Med 2009;50:1095–101.
[12] Kuhnast B, Damont A, Hinnen F, Catarina T, Demphel S, Le Helleix S, et al. [18 F]DPA-714, [18 F]PBR111 and [18 F]FEDAA1106-selective radioligands for imaging TSPO 18 kDa with PET: automated radiosynthesis on a TRACERLAb FX-FN synthesizer and quality controls. Appl Radiat Isot 2012;70:489–97.
[13] Damont A, Boisgard R, Kuhnast B, Lemee F, Raggiri G, Scarf AM, et al. Synthesis of 6-[(1)(8)F]fluoro-PBR28, a novel radiotracer for imaging the TSPO 18 kDa with PET. Bioorg Med Chem Lett 2011;21:4819–22.
[14] Wadsworth H, Jones PA, Chau WF, Durrant C, Fouladi N, Passmore J, et al. [18 F]GE-180: a novel fluorine-18 labelled PET tracer for imaging translocator protein 18 kDa (TSPO). Bioorg Med Chem Lett 2012;22:1308–13.
[15] Wadsworth H, Jones PA, Chau WF, Durrant C, Morisson-Iveson V, Passmore J, et al. Exploration of the structure-activity relationship of the diaryl anilide class of ligands for translocator protein–potential novel positron emitting tomography imaging agents. Bioorg Med Chem Lett 2012;22:5795–800.
[16] O'Shea D, Ahmad R, Arstad E, Avory M, Chau WF, Durrant C, et al. Exploration of the structure-activity relationship of a novel tetracyclic class of TSPO ligands-potential novel positron emitting tomography imaging agents. Bioorg Med Chem Lett 2013;23:2368–72.
[17] Freedman TB, Cao X, Dukor RK, Nafie LA. Absolute configuration determination of chiral molecules in the solution state using vibrational circular dichroism. Chirality 2003;15:743–58.
[18] Slovakova A, Hutt AJ. Chiral compounds and their pharmacologic effects. Ceska Slov Farm 1999;48:107–12.
[19] Nguyen LA, He H, Pham-Huy C. Chiral drugs: an overview. Int J Biomed Sci 2006;2:85–100.
[20] Morisson-Iveson V, Wadsworth H, Passmore J, Ewan A, Nilsen S, Thaning M, et al. An improved, regioselective synthesis of the radiolabelling precursor for the translocator protein targeting positron emission tomography imaging radiotracer [18 F]GE-180. Tetrahedron Lett 2014;55:5141–3.
[21] Taylor LT. Supercritical fluid chromatography for the 21st century. J Supercrit Fluids 2009;47:566–73.
[22] Le Fur G, Vaucher N, Perrier ML, Flamier A, Benavides J, Renault C, et al. Differentiation between two ligands for peripheral benzodiazepine binding sites, [3H]RO5-4864 and [3H]PK 11195, by thermodynamic studies. Life Sci 1983;33:449–57.
[23] Pike VW. PET radiotracers: crossing the blood-brain barrier and surviving metabolism. Trends Pharmacol Sci 2009;30:431–40.
[24] Kam WW, Meikle SR, Zhou H, Zheng Y, Blair JM, Seibel M, et al. The 18 kDa translocator protein (peripheral benzodiazepine receptor) expression in the bone of normal, osteoprotegerin or low calcium diet treated mice. PLoS One 2012;7:e30623.
[25] McAfee JG, Subramanian G. Interpretation of interspecies differences in the biodistribution of radioactive agents. Int J Nucl Med Biol 1983;10:48.